Bulletin of the Seismological Society of America, Vol. 96, No. 2, pp. 678–696, April 2006, doi: 10.1785/0120050056

Development of a Time-Domain, Variable-Period Surface-Wave Magnitude Measurement Procedure for Application at Regional and Teleseismic Distances, Part II: Application and M_s–m_b Performance

by Jessie L. Bonner, David R. Russell, David G. Harkrider, Delaine T. Reiter, and Robert B. Herrmann

Abstract The Russell surface-wave magnitude formula, developed in Part I of this two-part article, and the M_s(VMAX) measurement technique, discussed in this article, provide a new method for estimating variable-period surface-wave magnitudes at regional and teleseismic distances. The M_s(VMAX) measurement method consists of applying Butterworth bandpass filters to data at center periods between 8 and 25 sec. The filters are designed to help remove the effects of nondispersed Airy phases at regional and teleseismic distances. We search for the maximum amplitude in all of the variable-period bands and then use the Russell formula to calculate a surface-wave magnitude.

In this companion article, we demonstrate the capabilities of the method by using applications to three different datasets. The first application utilizes a dataset that consists of large earthquakes in the Mediterranean region. The results indicate that the M_s(VMAX) technique provides regional and teleseismic surface-wave magnitude estimates that are in general agreement except for a small distance dependence of -0.002 magnitude units per degree. We also find that the M_s(VMAX) estimates are less than 0.1 magnitude unit different than those from other formulas applied at teleseismic distances such as Rezapour and Pearce (1998) and Vaněk *et al.* (1962).

In the second and third applications of the method, we demonstrate that measurements of M_s(VMAX) versus m_b provide adequate separation of the explosion and earthquake populations at the Nevada and Lop Nor Test Sites. At the Nevada Test Site, our technique resulted in the misclassification of two earthquakes in the explosion population. We also determined that the new technique reduces the scatter in the magnitude estimates by 25% when compared with our previous studies using a calibrated regional magnitude formula. For the Lop Nor Test Site, we had no misclassified explosions or earthquakes; however, the data were less comprehensive.

A preliminary analysis of Eurasian earthquake and explosion data suggest that similar slopes are obtained for observed M_s(VMAX) versus m_b data with $m_b < 5$. Thus the data are not converging at lower magnitudes. These results suggest that the discrimination of explosions from earthquakes can be achieved at lower magnitudes using the Russell (2006) formula and the M_s(VMAX) measurement technique.

Introduction

The discrimination of small-to-intermediate magnitude ($3 < m_b < 5$) explosions and earthquakes remains a difficult problem for the nuclear monitoring community. For larger events, the relative difference between the body-wave (m_b) and surface-wave (M_s) magnitude for a seismic event is one of the best discriminant techniques available at teleseismic distances. The discriminant works because, at a given m_b, earthquakes usually generate substantially more surface-wave energy than explosions and thus are characterized by a larger surface-wave magnitude. Difference in focal mechanisms and the near-source material velocity also helps improve the discriminant performance (Stevens and Day, 1985). At regional distances, the measurement of surface-wave amplitudes is complicated because of nondispersed Airy phases. Hence, a remaining problem for the nuclear monitoring community is to create a seamless relationship

between estimating M_s at regional and teleseismic distances for events of a wider range of magnitudes.

Many of the surface-wave magnitude scales have been based on empirical formulas of the form:

$$M_s = \log A + B(\Delta) + C, \quad (1)$$

where A is the instrument-corrected ground motion measured in the time domain, usually in nanometers; $B(\Delta)$ is an attenuation term; and C is either a station correction, a term to scale for consistency between magnitude scales, or a path correction. These latter two terms are often determined empirically by averaging across many events at various distances.

The notion of using surface waves to obtain an estimate of source size was first introduced by Gutenberg (1945) using the equation:

$$M_s = \log A + 1.656 \log \Delta - 1.182 + S_c, \quad (2)$$

where A is the amplitude (in nanometers) of the horizontal ground motion at a period of 20 sec, and S_c is a station correction term. Vaněk *et al.* (1962) improved on this scale by developing a formula that could be used at periods in the vicinity of 20 sec over any epicentral distance. Thus for any distance Δ and period T approximately 20 sec, they proposed the formula:

$$M_s = \log(A/T) + 1.66 \log(\Delta) + 0.3. \quad (3)$$

At distances greater than 25 degrees, the M_s estimates from Gutenberg (1945) and Vaněk *et al.* (1962), also known as the Prague formula, agree within 0.2 magnitude units (m.u.) (Marshall and Basham, 1972). However, considerable problems arose, along with confusion in the literature, when the two scales were applied to both regional and teleseismic events. This led Marshall and Basham (1972) to reformulate the Vaněk *et al.* (1962) formula for use at regional and teleseismic distances; however, a path correction based on dispersion curves for shorter periods (<20 sec) was needed to account for Airy phase effects at these distances. Other improvements to empirical formulas have been developed by von Seggern (1977) and Herak and Herak (1993).

Recently, the trend has been to constrain surface-wave magnitude formulas to the theoretical aspects of surface-wave propagation, including dispersion, attenuation, and geometrical spreading. In the frequency domain, Kanamori and Stewart (1976) described the corrected amplitude (A_c) for a surface wave at distance Δ as:

$$A_c = A\sqrt{r_e \sin(\Delta)}\, e^{\frac{\pi\kappa\Delta}{UQT}}, \quad (4)$$

where A is the frequency domain amplitude, r_e is the radius of the earth, κ is the degrees to kilometers distance conversion term (111.2 km/deg), U is the group velocity at period T, and Q is the period-dependent quality factor. Okal (1989) used dispersion and attenuation relations to transform equation (4) into the time domain to compare a theoretical distance correction term with empirical terms in the Prague formula. Although the theoretical and empirical terms agreed favorably at distances between 20 and 100 degrees, discrepancies occurred at regional distances.

Rezapour and Pearce (1998) sought to reconcile these discrepancies by developing a new formula for M_s defined as:

$$M_s = \log \frac{A}{T} + \frac{1}{3}\log(\Delta) + \frac{1}{2}\log(\sin(\Delta)) + 0.0046\Delta + 2.370. \quad (5)$$

The Rezapour and Pearce (1998) equation was developed by using theoretical aspects of dispersion, including Airy phase propagation, as evidenced by the 1/3 coefficient on the dispersion term, and geometrical spreading. However, because they did not consider frequency-dependent aspects of dispersion, the coefficient is not sufficient to account for dispersion effects at shorter periods (Bonner *et al.*, 2003). The formula was adopted by the prototype International Data Center in 1998 for calculating surface-wave magnitudes at distances between 20 and 100 degrees; however, it is now used by the International Data Center to determine an M_s for all surface waves recorded at distances less than 100 degrees (Stevens and McLaughlin, 2001).

Russell (2006; Part I of this article) developed a time-domain method for measuring surface waves with minimum digital processing, using zero-phase Butterworth filters. The method can effectively measure surface-wave magnitudes at both regional and teleseismic distances, at variable periods between 8 and 25 sec. For applications over typical continental crusts, the magnitude equation is:

$$M_{s(b)} = \log(a_b) + \frac{1}{2}\log(\sin(\Delta)) + 0.0031\left(\frac{20}{T}\right)^{1.8}\Delta - 0.66\log\left(\frac{20}{T}\right) - \log(f_c) - 0.43, \quad (6)$$

where a_b is the amplitude of the Butterworth-filtered surface waves (zero-to-peak in nanometers) and $f_c \le 0.6/(T\sqrt{\Delta})$ is the filter frequency of a third-order Butterworth bandpass filter with corner frequencies $1/T - f_c$, $1/T + f_c$. At the reference period $T = 20$ sec, the equation is equivalent to von Seggern's formula (1977) scaled to Vaněk *et al.* (1962) at 50 degrees. For periods $8 \le T \le 25$ sec, the equation is corrected to $T = 20$ sec, accounting for source effects, attenuation, and dispersion.

The purpose of this article is to present the results of applying the Russell (2006) formula at teleseismic and regional distances for variable-period data. First, we applied the formula to a large earthquake dataset to demonstrate the analysis method and to determine whether the regional and

teleseismic magnitudes are unbiased with respect to each other. We compare the resulting magnitudes from the Russell equation with estimates from Vaněk *et al.* (1962) and Rezapour and Pearce (1998). Then, we used the formula to estimate surface-wave magnitudes for explosions and earthquakes in Eurasia and North America to examine if we could improve discrimination performance.

Methodology

The surface-wave magnitude estimation procedure currently employed at most data centers involves measuring the amplitude of surface waves near 20-sec period. In our past research projects (Bonner *et al.*, 2003), we tried to extend the magnitude estimation to shorter periods (e.g., 7 sec). We determined that shorter-period surface waves could be used for magnitude estimation for events with smaller m_b values. Although the 7-sec magnitude scale formed a robust discriminant at the Nevada Test Site (NTS), it failed to provide adequate explosion/earthquake separation at other test sites where the earthquakes were deeper than typical NTS events. This was a primary factor in the development of a measurement technique for variable periods (between 8 and 25 sec) and magnitude estimation using the Russell (2006) formula. We refer to this technique as VMAX for Variable-period, MAXimum amplitude estimates. In the following paragraphs, we describe how we positively identify Rayleigh wave motion and apply this new magnitude estimation technique.

Surface-Wave Identification

The largest amplitudes of near-regional surface waves for shallow events in North America and Eurasia typically occur at periods less than 20 sec, and these amplitudes can often be 6–10 dB larger than the amplitudes measured at the 20-sec period. Therefore, M_s scales that consider variable-period surface waves will be applicable to lower m_b values. Note that caution must be used to ensure that the measured signals are, in fact, Rayleigh waves and not microseisms, higher-mode energy, or Love wave contamination.

After correcting for the instrument response, we employ a surface-wave processing routine that is designed to positively identify small amplitude, fundamental-mode, Rayleigh-wave motion. The method is applied to all events with $m_b < 4.0$, because the signal-to-noise ratio (SNR) for larger events is great enough that amplitude measurements can be made by bandpass filtering the velocity records and measuring the amplitudes in a group velocity window indicative of surface waves (2–4 km/sec). Note that this technique can be fully automated in an operational setting so that events of all magnitudes will utilize the same processing technique.

For events with $m_b < 4.0$, we first use the multiple-filter analysis technique (Dziewonski *et al.*, 1969) to generate a group velocity dispersion curve for each event-to-station path. We then overlay the theoretical fundamental- and first-higher mode dispersion curves predicted for the path from the Stevens *et al.* (2001) global shear-wave model. We require overlap (similar to Stevens and McLaughlin, 2001) in the observed dispersion, plus error in the 8- to 25-sec period band, with the predicted fundamental-mode dispersion from the Stevens *et al.* (2001) model.

If the event passes the dispersion test, we then determine whether the signal has retrograde elliptical particle motion and a backazimuth that is within ± 30 degrees of the true backazimuth. We have followed the methods of Chael (1997) and Selby (2001) to determine the backazimuth that corresponds to the largest positive value, indicative of retrograde elliptical motion, in a covariance matrix formed by the Hilbert-transformed vertical component and the two horizontal components. If a given event passes the dispersion, backazimuth, and particle motion tests, we feel that we have positively identified fundamental-mode Rayleigh waves for the event of interest.

Butterworth Filtering

Once we have positively identified the fundamental-mode Rayleigh waves, we apply a series of zero-phase third-order Butterworth filters to the data with the corner frequencies $1/T - f_c$, $1/T - f_c$, where $f_c \leq 0.6/(T\sqrt{\Delta})$. The center periods are placed at 1-sec intervals between 8 and 25 sec. We note that increasing this interval to 3 sec or lowering it to 0.1 sec will typically result in less than a 0.05-m.u. change in the resulting magnitude. We construct the envelope function of the filtered signal and measure the maximum zero-to-peak amplitude in a group velocity window between 2.0 and 4.0 km/sec. An analyst then visually confirms that the correct waveform feature is being measured—a benefit of using a time-domain measurement.

In Figure 1 we show examples of filter panels from four stations that recorded an m_b 5.5 Dodecanese Islands event in August 2004. These four examples highlight characteristics of Rayleigh waves at regional and teleseismic distances that must be considered when developing a variable-period formula at both distances. The Russell (2006) formula has been developed to account for these differences in the excitation, attenuation, and propagation of variable-period surface waves.

For example, station LAST is located only 263 km from the event's epicenter, and its largest surface-wave amplitude occurs at a period of 8 sec. Note that the relative amplitudes for the 20-sec surface waves, where typical surface-wave measurements are estimated, are much smaller than the 8-sec period waves. If the event had been significantly smaller than m_b 5.5, the 20-sec surface waves could have disappeared below the noise level prior to the 8-sec data, and a standard M_s measurement would have been impossible to estimate.

However, we point out that even though the maximum amplitude for station LAST is visually observed at a period of 8 sec in the first subplot of Figure 1, an 8-sec period may

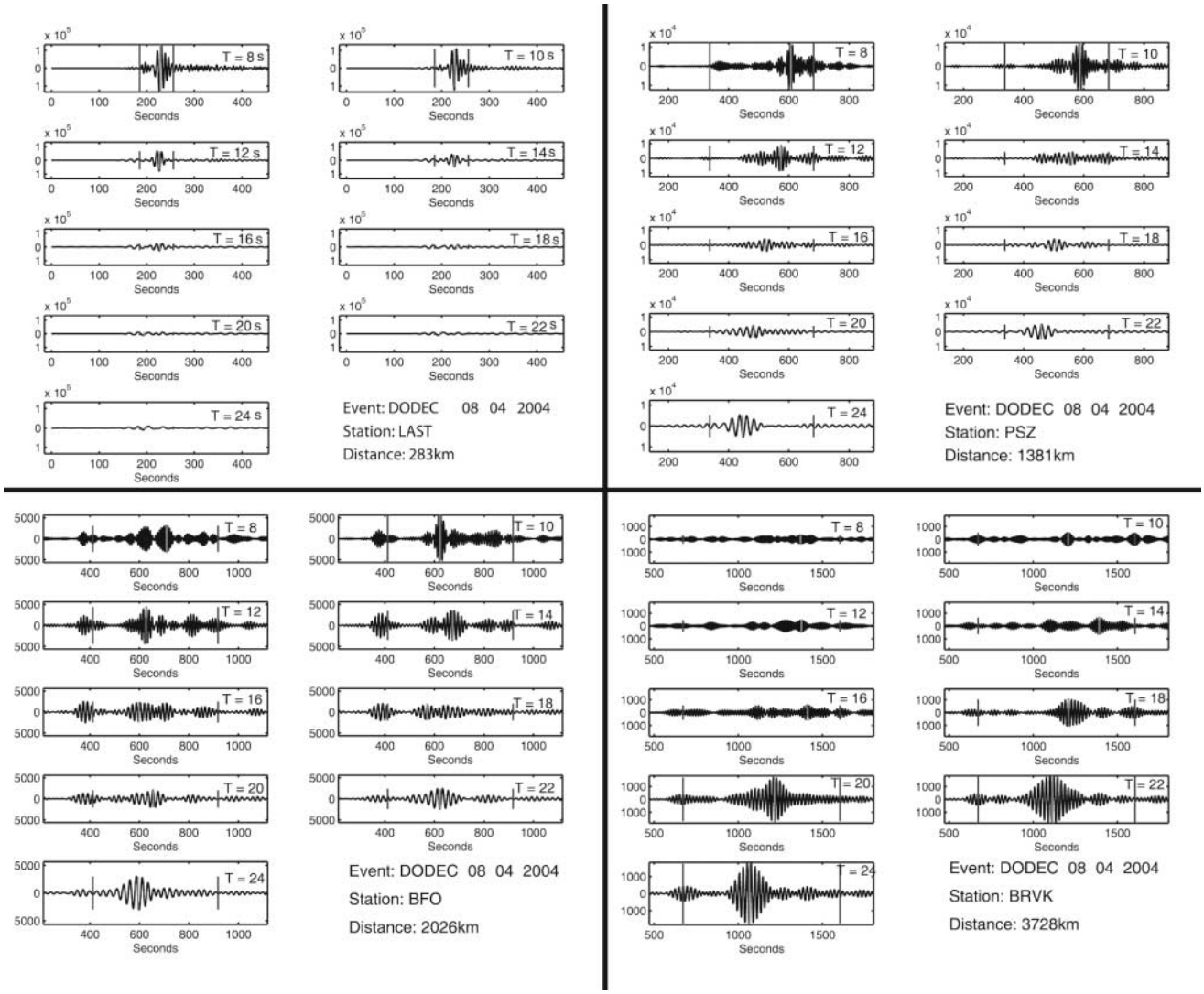

Figure 1. Examples of Butterworth-filtered seismograms for a Dodecanese Islands event recorded at LAST, PSV, BFO, and BRVK. In each subplot, the *y* axis is presented with the same amplitude scale. The *x* axis is time in seconds from the event origin. Each filter panel has two vertical lines that represent group velocity windows of 2.0 and 4.0 km/sec. The location of the maximum amplitude at each center period is also marked by a thin vertical line.

not be considered when we average stations for a final magnitude (as discussed in the following section of this article). This is because the bandwidth chosen for filtering varies according to the formula $f_c \leq 0.6/(T\sqrt{\Delta})$, to remove the effects of Airy phases. To correct the variable bandwidth to equivalent spectral amplitudes and thus get the true period of the maximum amplitude, the log amplitude data must be corrected by using a $\log(f_c)$ factor. Note that the same amplitude-correction effect is taken into account in equation (6) for magnitude estimation. We find that amplitude correction at station LAST results in a maximum amplitude at a period of 9 sec, which is the period used to form a network average magnitude.

For station PSZ at 1,381 km, the largest amplitude visually occurs at 8-sec period, and the amplitude difference between the filter bands decreases as the period increases. The decrease in the difference between the shorter- and longer-period surface waves results in a period of maximum Airy-corrected amplitude at 25 sec. After the surface waves have traveled 2026 km to BFO, the filtered amplitudes at periods of 10 sec are the largest for this event. After correction for the Airy phase filtering term, the period of maximum amplitude becomes 25 sec However, when the surface waves arrive at typical teleseismic distances (e.g., station BRVK at 3728 km), the largest amplitude surface waves (both visually and corrected) have a period of 23 sec.

Estimating the Magnitude

We record the maximum amplitude in each of the 18 filter bands and then use equation (6) to calculate a variable-period surface-wave magnitude. As noted in Figure 2, 18 different magnitudes are estimated for each station recording the event. For operational purposes, the technique will be simplified to search for the maximum corrected amplitude over all filter bands, thus reducing the number of magnitudes to be calculated from 18 to 1. However, for research purposes, it helps to understand the method to calculate magnitudes for each filter band.

We tried several different techniques to determine the final magnitude from the analysis of surface-wave data presented in Figure 2. For instance, for the M_s(VMAX) technique, we search the variable-period filtered data to determine the period of the maximum Airy-corrected amplitude. Then we use the uncorrected amplitude at that period for the final magnitude estimation. We use the uncorrected amplitude because of the $\log(f_c)$ term in equation (6). The black large solid circles in Figure 2 show the period of the maximum Airy-corrected amplitudes and the magnitudes for the filtered data shown in Figure 1. In addition to the M_s(VMAX) technique, we have also studied a maximum-magnitude technique in which we determine the maximum magnitude over all the estimates in Figure 2. Using this method we determined that there was 0.02 magnitude unit increase in the average values.

In another comparison, we calculated a mean magnitude using the magnitude estimates from the 8- to 25-sec period band; however, this technique did not work when holes in the earthquake spectra were encountered or when the higher-frequency data were attenuated at teleseismic distances. As shown in Figure 2, the shorter-period data for station BRVK have been attenuated. Our results will be improperly biased if we average the estimates over the 18 periods. In contrast, by using the period of maximum Airy-corrected amplitude in the M_s(VMAX) formula, we are able to diminish any influence that spectral holes or attenuation effects may have in the magnitude estimation.

As noted in the introduction, another goal of this article is to demonstrate that the M_s(VMAX) formula is valid for both the regional and teleseismic surface-wave estimates. A regression of the estimates with epicentral distance shows that there is a 0.001-m.u. decrease per degree for these four stations that recorded this Dodecanese event on both regional (LAST and PSV) and teleseismic stations (BFO and BRVK).

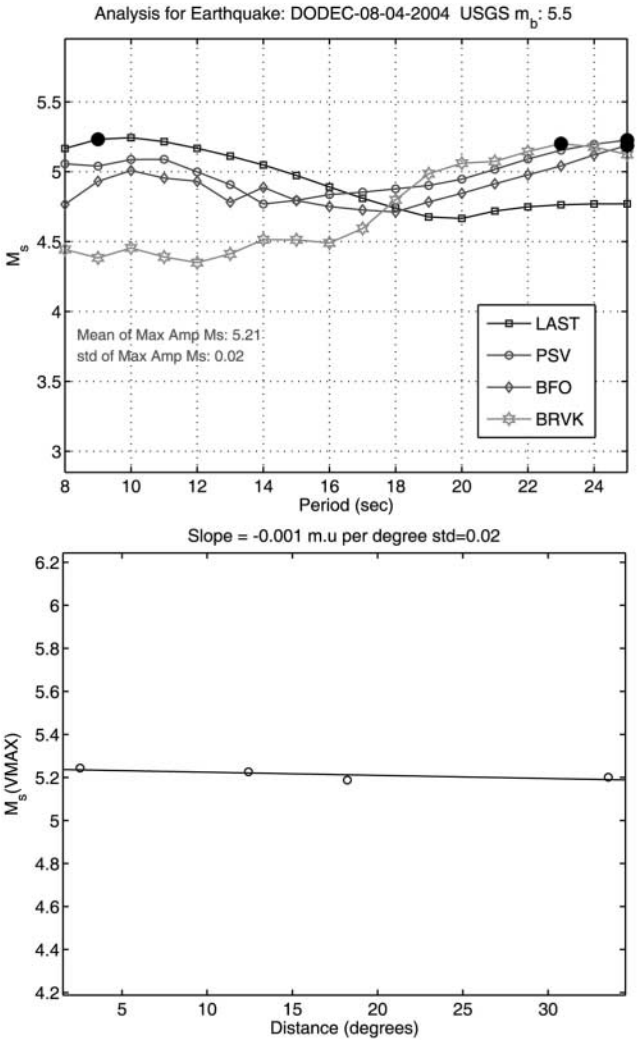

Figure 2. (Top) Example of the magnitude estimation technique M_s(VMAX) for the Butterworth bandpass-filtered data shown in Figure 1. The symbols show the magnitudes estimated using equation (6) at each center period. The larger filled circles show the period of maximum amplitude for the filtered seismic data corrected by a $\log(f_c)$ term, and the average and standard deviation of these four estimates are provided. (Bottom) Linear regression of the magnitudes versus distance for the four estimates in the top subplot.

Excitation Correction

The source spectra for Rayleigh waves generated from shallow explosions will typically be enriched in short-period surface wave energy. Thus the term $0.66 \log(20/T)$ in equation (6) is a source excitation correction. The correction was determined by considering synthetics generated from nuclear explosions at 1 km depth in various crustal velocity structures (as discussed in Bonner *et al.*, 2004). We apply the correction to all events even though it was developed with a shallow explosion assumption. This is essentially the same procedure as Stevens and McLaughlin (2001), except that they used spectral instead of time-domain measurements and derived the source and receiver functions from earth models.

To illustrate the effect of the corrections on our data, we present the M_s(VMAX) analysis of three near-regional recordings of NTS explosions (Fig. 3). The upper plot shows the magnitudes calculated by using the same techniques pre-

sented in Figure 2 (e.g., using equation 6). We have applied the excitation correction to these data and determined the magnitude to be 4.13. However, in the lower plot, we did not apply the excitation correction and the enriched short-period energy for the nuclear explosion is evident. We have estimated a magnitude of 4.38 for these uncorrected data, which represents a 0.25-m.u. increase over the corrected results. Using the uncorrected estimate would result in decreased effectiveness of the M_s–m_b discriminant.

The goal of the excitation correction is to flatten the explosion M_s curves across the various periods. We are approaching that goal in Figure 3 for near-regional recordings of NTS explosions. To improve on corrections in other regions, we could use empirically determined source corrections measured from previous explosions. For this initial test of the method, we have chosen to remain with one standard global correction as opposed to station-specific corrections. That could be considered in the future to further reduce variances in the estimates.

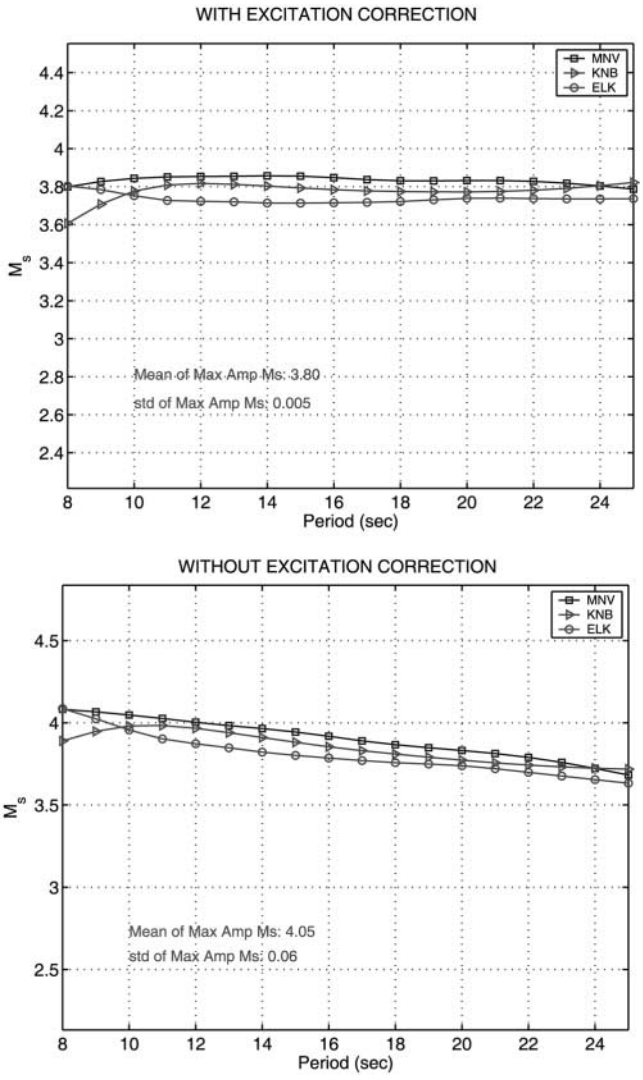

Figure 3. (Top) Example of the magnitude estimation technique M_s(VMAX) for the NTS explosion Cabra. The excitation correction 0.66 log(20/T) was applied to these magnitude estimates. (Bottom) Estimated M_s(VMAX) without applying an excitation correction.

Application

We applied the Russell (2006) formula and our M_s(VMAX) technique to three different surface-wave datasets. For the first application of the formula, we estimated surface-wave magnitudes for several large earthquakes in the Mediterranean region of Europe. For the second and third applications, we estimated M_s(VMAX) for earthquakes and explosions in North America and Eurasia, respectively. And finally, we examined all the data in Eurasia to determine the performance of the M_s–m_b discriminant when our magnitude estimation techniques are used.

Mediterranean Region

We applied the Russell (2006) formula and M_s(VMAX) measurement technique to earthquakes in the Mediterranean region to determine whether (1) we obtain consistent magnitudes at regional and teleseismic distances and (2) our M_s estimates match those obtained using the Vaněk *et al.* (1962) and Rezapour and Pearce (1998) formulas.

Data. We developed a database of broadband recordings of 33 earthquakes that occurred in the Mediterranean region of Europe (Fig. 4 and Table 1). For this pilot study, we

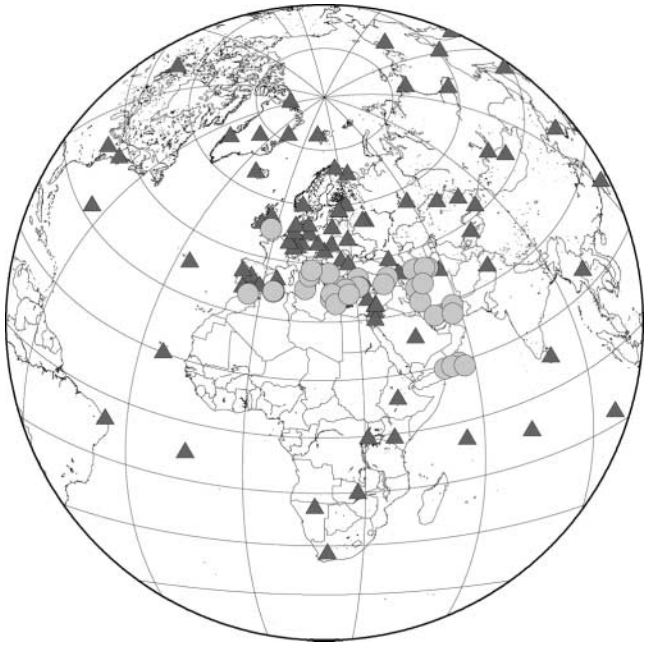

Figure 4. Test dataset of events in the Mediterranean region and stations used to test the Russell (2006) formula and M_s(VMAX) measurement technique.

Table 1
Origin Information and M_s(VMAX) Test Results for Events in the Mediterranean Region

Year	Month	Day	Hour	Minute	Second	Latitude	Longitude	Depth	m_b	M_s (VMAX)	STD	No.
2004	08	04	3	1	07	36.92	27.76	10	5.5	5.21	0.02	44
2004	08	11	15	48	21	38.38	39.25	10	5.5	5.54	0.17	41
2004	05	28	0	38	44	36.25	51.62	17	6.3	6.34	0.20	58
2004	05	28	12	38	46	36.27	51.57	26	6.2	6.30	0.19	46
2004	03	01	0	36	02	37.22	22.26	31	5.5	4.45	0.19	36
2004	03	17	5	21	01	34.59	23.48	25	6.1	5.71	0.2	42
2004	03	25	19	30	50	39.93	40.86	10	5.5	5.30	0.19	45
2004	01	14	16	58	51	27.7	52.31	33	5.4	4.34	0.21	34
2004	01	28	9	6	06	26.89	57.59	10	5.4	4.57	0.23	38
2004	02	13	0	41	40	13.69	57.25	10	5.5	4.86	0.24	35
2004	02	24	2	27	46	35.14	−4	0	6.4	6.3	0.22	42
2003	12	26	3	6	17	28.86	58.32	33	5.4	5.31	0.17	39
2003	05	24	1	46	06	14.43	53.81	10	5.8	5.49	0.23	47
2003	04	10	0	40	15	38.21	26.87	10	5.6	5.41	0.18	33
2003	05	27	17	11	29	36.94	3.58	8	5.7	5.21	0.25	49
2003	03	29	17	42	18	43.26	15.49	33	5.5	5.14	0.24	34
2002	10	31	10	32	59	41.73	14.89	10	5.6	5.45	0.18	29
2002	09	06	1	21	28	38.37	13.72	10	6.1	5.63	0.2	26
2002	09	25	22	28	16	32.09	49.23	33	5.5	5.00	0.22	28
2002	08	13	8	37	23	14.75	55.85	10	5.8	5.49	0.26	49
2002	09	01	17	14	59	14.25	51.81	10	5.6	5.80	0.25	28
2002	04	24	10	51	51	42.43	21.51	10	5.5	5.42	0.19	23
2002	06	22	2	58	21	35.63	49.05	10	6.5	6.33	0.18	59
2002	04	17	8	47	22	27.61	56.76	33	5.4	4.62	0.20	39
2002	02	03	7	11	28	38.57	31.27	5	6.5	6.38	0.22	65
2002	02	03	9	26	43	38.63	30.9	10	5.8	5.48	0.22	68
2001	07	26	0	21	38	39.06	24.34	10	6.3	6.66	0.18	12
2001	06	10	1	52	08	39.84	53.89	34	5.6	5.00	0.25	21
2000	11	25	18	9	11	40.25	49.95	50	6.3	6.55	0.16	48
2000	12	06	17	11	06	39.57	54.8	30	7	7.3	0.28	69
2000	12	15	16	44	45	38.61	31.06	10	5.8	5.62	0.13	15
2000	05	24	5	40	38	36.04	22.01	33	5.7	5.57	0.16	51
1999	11	12	16	57	20	40.76	31.16	10	7.2	7.35	0.25	55

focused on larger events (m_b >5.4) with depths of 50 km or less. These restrictions ensured adequate SNRs for the surface waves recorded at regional and teleseismic distances. The data were acquired from the Incorporated Research Institutions for Seismology (IRIS) and consisted of global and regional networks in the study region. The data were all transformed from counts to displacement in nanometers by using the Seismic Analysis Code command "transfer" and the SEED response files. The data were decimated from their original sampling rates (>20 samples/sec) to approximately 1 sample/sec for the surface-wave analysis. Down-sampling increases the analysis speed and eliminates digital filter problems associated with narrow-band filtering, as discussed in the electronic supplement of Russell (2006).

Results. Table 1 provides the M_s(VMAX) values obtained for the earthquakes in the Mediterranean region. Our first objective in this exercise was to determine whether there is a distance dependence in the formula and measurement technique. As mentioned in the introduction, previous research has been unsuccessful at finding a single, variable-period formula valid at both regional and teleseismic distances.

We performed a distance analysis on all 33 events of our test database similar to the one performed in the lower plot of Figure 2. To compare events of different magnitudes, we removed the mean magnitude from each event's analysis. Figure 5 shows the results, which include 1318 M_s(VMAX) magnitude estimates from the events listed in Table 1. Our objective was to test the formula for a predominance of continental paths; thus, data are at distances less than 70 degrees. A linear regression of the mean-removed magnitude estimates with increasing distance shows a small (0.002 m.u. per degree) decrease in magnitudes. The standard deviation for the regression analysis is 0.21 m.u. This suggests that if an event had an M_s(VMAX) magnitude estimate of 6.0 measured at a distance of 5 degrees, the magnitude estimated at a distance of 60 degrees would be ~5.89. This difference is well within the scatter typically observed for surface-wave magnitude estimates resulting from focal mechanisms and path effects.

Because M_s(VMAX) is a variable-period technique, we

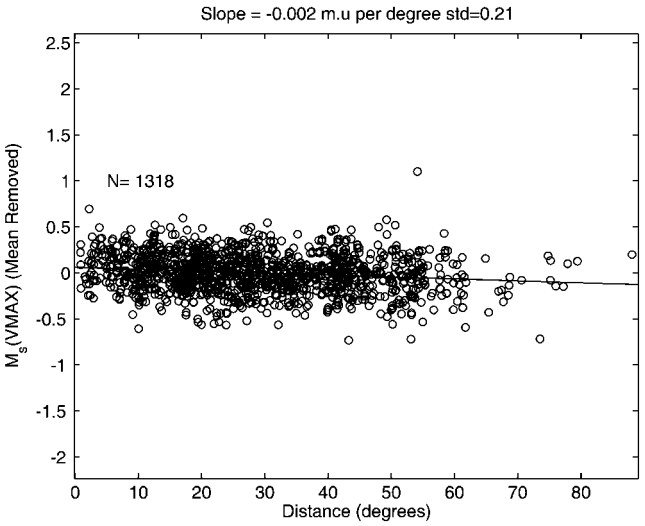

Figure 5. Regression of mean-removed M_s(VMAX) magnitude estimates for the 33 events in Table 1 with distance. There is a very small decrease in magnitude units (0.002 m.u. per degree) with increasing distance.

also examined the periods at which the estimates were formed (Fig. 6). There is a general increase in the number of measurements in each bin from shorter to longer periods. This increase is reassuring, because it is consistent with past studies which found that the best period range to measure M_s is between 17 and 23 sec.

We observe an edge effect associated with ending the surface-wave magnitude analysis at 25 sec. Two explanations exist for this behavior. Because of their spectral shape, the earthquakes will tend to select longer periods, especially when the events are deeper than the upper crust. In addition, because of the nature of surface-wave propagation, we would expect to see a general trend of longer-period measurements with increasing distances. This trend is related to the rapid attenuation of shorter-period amplitudes compared with the longer periods at longer epicentral distances. In Figure 6, we plotted the distances and periods at which the magnitudes were estimated. The plot shows that for the magnitudes estimated at periods of 10 sec or less, the corresponding epicentral distances were less than 30 degrees. From 10 to 18 sec, we note a general increase in the cut-out distance from 30 to 60 degrees. For periods greater than 18 sec, note that the cutout distance continues to increase but is less constrained by the available data. The results in Figure 6 suggest that the formula is behaving as we intended. It also hints that the analysis could be improved by increasing the long-period limit to periods greater than 25 sec.

As a final step in the analysis of the events in Table 1, we compared our M_s(VMAX) estimates with magnitude estimates published by the U.S. Geological Survey (USGS) and the International Data Center (IDC) in Vienna, and with the M_w estimates obtained from Harvard's Centroid Moment Tensor (CMT) analysis. The results are shown in Figure 7. Note that the USGS uses the Vaněk *et al.* (1962) formula, whereas the IDC uses the Rezapour and Pearce (1998) formula. We performed a fixed-slope (slope $= 1$) regression of the M_s(VMAX) estimates against the results from the other organizations to determine the offset between the estimates. The results indicate that the M_s(VMAX) is -0.03 and 0.05 m.u. different than the Vaněk *et al.* (1962) and Rezapour and Pearce (1998) formulas, respectively. Differences of this size for all three comparisons are well within the scatter of the observations. Also, the bottom subplot of Figure 7 shows that the M_s(VMAX) and M_w estimates are approximately equal for $6.0 < M_w < 7.2$.

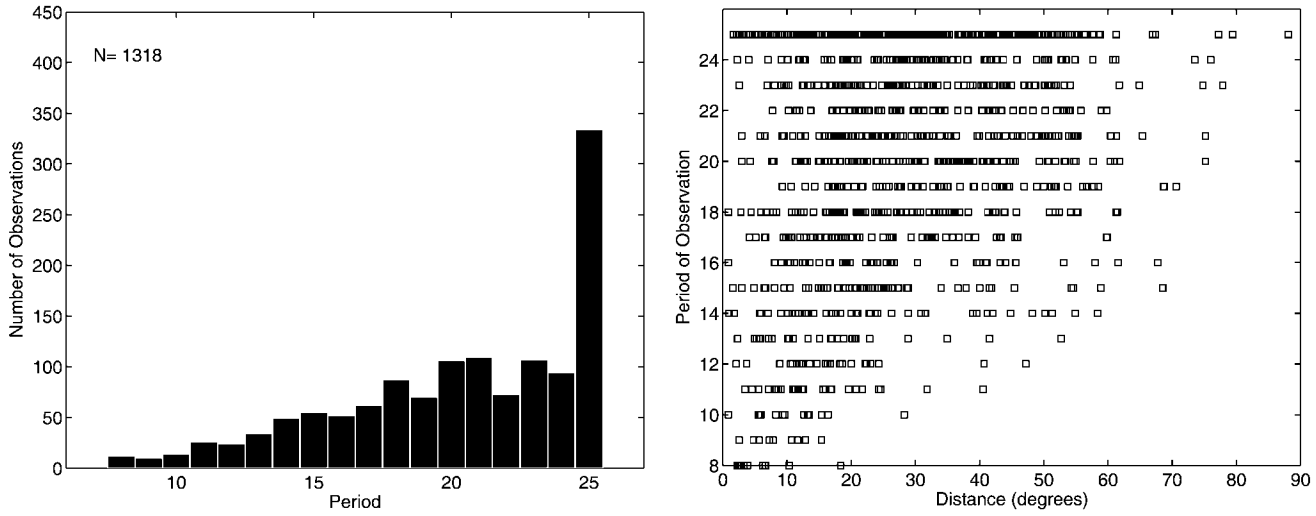

Figure 6. (Left) Bins showing the periods used to estimate the M_s(VMAX) magnitudes at 1318 different station-source pairs. (Right) Comparison of the periods of the M_s(VMAX) estimates compared with the epicentral distance.

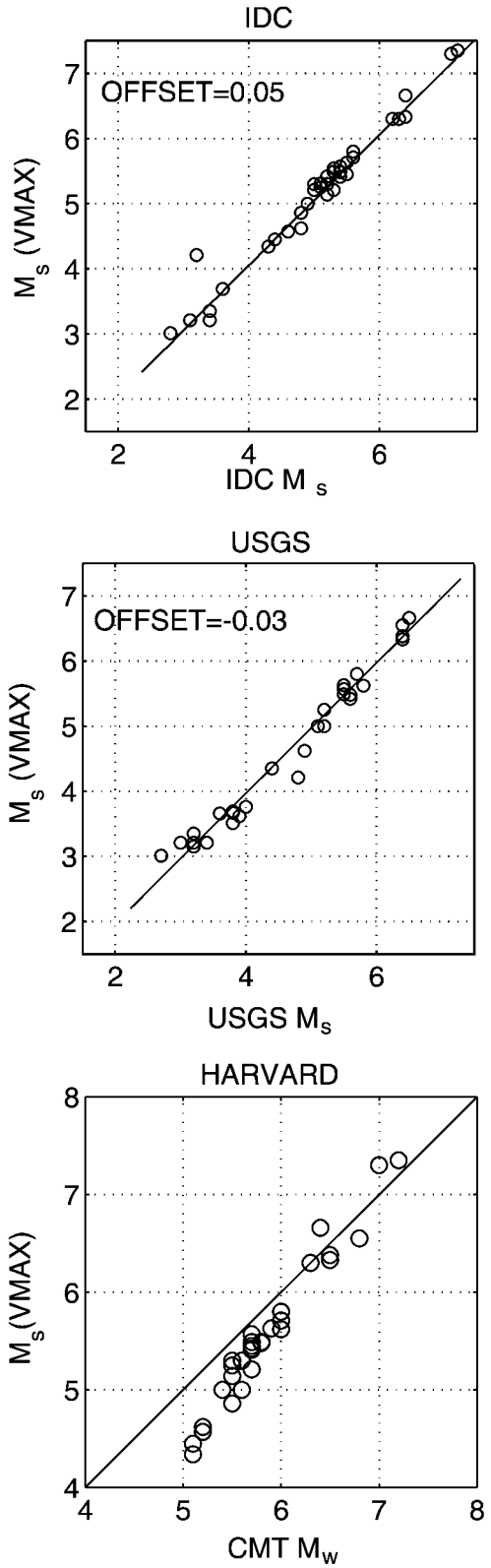

Figure 7. (Top) Fixed-slope (slope = 1) regression of M_s(VMAX) network-average magnitudes versus the IDC M_s for the Mediterranean events. (Middle) Fixed-slope (slope = 1) regression of M_s(VMAX) network-average magnitudes versus the USGS M_s. (Bottom) Comparison of the M_s(VMAX) network-average magnitudes versus the Harvard CMT M_w values.

Nevada Test Site Earthquake and Explosion Discrimination

We next examined the performance of the Russell (2006) formula and M_s(VMAX) measurement technique on earthquake and explosion discrimination at the Nevada Test Site in the western United States.

Data. We developed a test dataset consisting of explosions and earthquakes in the western United States. The explosion data are digital broadband seismograms from NTS explosions recorded on two or more stations of the Lawrence Livermore Regional Seismic network (henceforth referred to as LNN). The LNN network consists of seismic stations at Landers, California (LAC); Mina, Nevada (MNV); Elko, Nevada (ELK); and Kanab, Utah (KNB); it has been in operation since the 1960s (Fig. 8). All data were converted from counts to displacement in nanometers using the Seismic Analysis Code (SAC) "transfer" command and pole-zero files.

We estimated M_s(VMAX) for NTS explosions that occurred between December 1968 and September 1992. Our primary focus was on the 198 NTS explosions that were detonated after August 1979, when digital data became available from the LNN stations. Of these 198 events, 133 had useable data, of which 65 either had no available LNN data, were plagued by untimely data dropouts and glitches, or were too small for measurable surface-wave energy. We also analyzed 21 explosions detonated prior to July 1979 that were digitized from analog records, to compare our new re-

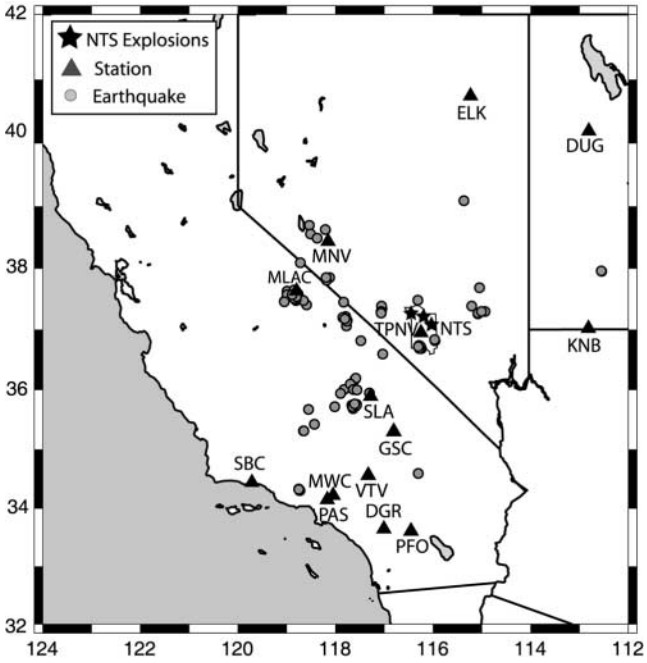

Figure 8. Test dataset consisting of NTS explosions recorded on the LNN dataset together with earthquakes in the western United States recorded on at least one LNN station and other regional networks.

sults with previous M_s studies completed by Yacoub (1983) and Woods and Harkrider (1995). In addition to the explosion dataset, we also estimated the M_s and m_b magnitudes for 69 earthquakes whose locations are shown as gray circles in Figure 8. These events were recorded on various networks in the region; however, we ensured that at least one LNN station recorded the event. This requirement allowed us to measure an unbiased m_b using the Denny *et al.* (1987, 1989) *Pn* magnitude scale. Many of the m_b(*Pn*) values used in this study were taken from Vergino and Mensing (1989) or Patton (2001).

Results. Table 2 provides the M_s(VMAX) estimates and standard deviations for the explosions on the Nevada Test Site. We compared the M_s(VMAX) measurements for the 154 explosions to the single 7-sec period measurements from our previous research. Figure 9 shows that the M_s(VMAX) explosion magnitudes are approximately 0.23 m.u. larger than the regionally calibrated Marshall and Basham M_s (7) estimates from Bonner *et al.* (2003). The slope of the best-fit line between the two datasets is approximately equal to 1. The M_s(VMAX) methodology resulted in a 25% reduction of the variance for the explosions over the previous single-period techniques.

An important goal of our research is the ability to estimate near-regional M_s values for NTS events that can be calibrated to conventional M_s scales. Figure 10 shows the comparison of our M_s(VMAX) estimates, which are taken directly from the regional surface waves, to M_s measurements obtained from a modeling technique derived by Woods and Harkrider (1995) and to estimates from far-regional/teleseismic data (Yacoub, 1983). Woods and Harkrider modeled the surface waves recorded at regional distances and then propagated the regional synthetics to distances of 40 degrees. At 40 degrees, their synthetics displayed significant 20-sec surface-wave energy, and the authors used a modified von Seggern (1977) formula to measure M_s from the synthetics. We performed a fixed-slope (slope = 1) linear regression to compare the M_s(VMAX) values with the Woods and Harkrider (1995) values and found a strong correlation. The offset shows that the M_s(VMAX) estimates are -0.11 m.u. lower than the Woods and Harkrider (1995) estimates.

We also compared the M_s(VMAX) estimates with teleseismic M_s estimates from Yacoub (1983). The results, shown in Figure 10, indicate that the two magnitude scales have similar scaling relationships, based on the fixed-slope regression analysis. In this case, the M_s(VMAX) estimates are offset from Yacoub's (1983) estimates by approximately $+0.03$ m.u.

Figure 11 shows the regression of the M_s(VMAX) versus the Denny *et al.* (1987, 1989) m_b for both the earthquake (Table 3) and explosion (Table 2) populations in our test dataset. The best-fitting regression lines are plotted as solid lines, and the slope and intercepts for the lines are presented in the left subplot. The populations plotted in Figure 11 sug-

Table 2
M_s(VMAX) Test Results for Explosions on the Nevada Test Site

Date	Name	m_b	M_s (VMAX)	STD	No.
1968354	Benham	6.49	5.88	0.21	3
1969302	Calabash	5.5	4.46	0.05	2
1970085	Handley	6.57	5.78	0.04	4
1970146	Flask	5.47	4.17	0.09	4
1970351	Carpetbag	5.79	4.69	0.14	4
1972265	Osocurro	5.6	4.47	0.06	3
1972270	Delphinium	4.54	2.69	0.08	3
1973116	Starwort	5.49	4.05	0.04	4
1973157	Alemendro	6.23	5.33	0.19	3
1974191	Escabosa	5.54	4.59	0.04	2
1975059	Topgallant	5.7	4.44	0.05	4
1975154	Stilton	6.03	4.77	0.06	4
1975154	Mizzen	5.66	4.52	0.03	4
1975170	Mast	6.24	5.18	0.12	4
1975324	Inlet	6.01	5.03	0.13	4
1975354	Chiberta	5.76	4.62	0.05	4
1976035	Keelson	5.61	4.41	0.04	4
1976035	Esrom	5.69	4.59	0.06	3
1976045	Cheshire	6.13	5.18	0.07	4
1976069	Estuary	6.09	5.25	0.13	4
1976077	Strait	5.87	4.81	0.09	3
1979215	Burzet	4.78	3.14	0.08	3
1979220	Offshore	4.85	3.38	0.04	3
1979241	Nessel	4.93	3.41	0.14	4
1979249	Hearts	5.83	4.67	0.02	4
1979269	Sheepshead	5.73	4.60	0.05	4
1980059	Tarko	4.43	3.12	0.16	3
1980094	Liptauer	4.9	3.15	0.28	4
1980107	Pyramid	5.45	4.28	0.20	4
1980117	Colwick	5.66	4.60	0.05	4
1980123	Canfield	4.38	2.84	0.03	3
1980164	Kash	5.61	4.67	0.04	3
1980176	Huron King	4.2	2.45	0.10	3
1980207	Tafi	5.8	4.70	0.05	4
1980213	Verdello	4.12	2.67	0.14	2
1980269	Bonarda	4.5	2.44	0.16	4
1980298	Dutchess	4.43	3.00	0.12	4
1980305	Miners Iron	4.65	3.34	0.12	4
1980319	Dauphin	4.39	3.01	0.07	4
1980352	Serpa	5.26	4.05	0.06	4
1981015	Baseball	5.56	4.41	0.02	4
1981149	Aligote	4.19	2.75	0.06	3
1981157	Harzer	5.62	4.42	0.09	4
1981191	Niza	4.18	2.58	0.06	4
1981239	Islay	3.96	2.40	0.03	2
1981247	Trebbiano	3.98	2.12	0.11	4
1981274	Paliza	5.12	3.80	0.01	3
1981315	Tilci	4.9	3.41	0.12	4
1981316	Rousanne	5.38	4.17	0.05	4
1981337	Akavi	4.7	3.23	0.18	4
1981350	Caboc	4.53	2.80	0.10	4
1982028	Jornada	5.76	4.65	0.04	4
1982043	Molbo	5.48	4.42	0.15	4
1982043	Hosta	5.76	4.45	0.06	4
1982107	Tenaja	4.49	2.95	0.09	4
1982115	Gibne	5.47	4.42	0.04	4
1982126	Kryddost	4.19	2.48	0.06	2
1982127	Bouschet	5.66	4.28	0.05	4
1982167	Kesti	4.01	2.33	0.03	3
1982175	Nebbiolo	5.73	4.57	0.09	4

(*continued*)

Table 2
Continued

Date	Name	m_b	M_s (VMAX)	STD	No.
1982210	Monterey	4.68	2.86	0.23	4
1982217	Atrisco	5.82	4.71	0.07	4
1982266	Frisco	4.9	3.49	0.13	3
1982266	Huron Landing	4.88	3.35	0.11	3
1982316	Seyval	4.18	2.35	0.01	2
1982344	Manteca	4.72	3.10	0.10	4
1983085	Cabra	5.36	4.12	0.04	3
1983104	Turquoise	5.64	4.18	0.05	4
1983112	Armada	4.15	2.33	0.25	3
1983125	Crowdie	4.37	2.65	0.09	3
1983146	Fahada	4.52	3.21	0.07	4
1983160	Danablu	4.73	2.80	0.02	2
1983215	Laban	4.48	2.59	0.14	2
1983223	Sabado	4.17	2.46	0.18	3
1983239	Jarlsberg	3.87	2.27	0.20	2
1983244	Chancellor	5.52	4.22	0.11	3
1983264	MidniteZ	4.04	2.66	0.21	4
1983265	Techado	4.2	2.48	0.08	4
1983350	Romano	4.97	3.77	0.07	3
1984031	Gorbea	4.51	2.79	0.11	4
1984061	Tortugas	5.82	4.51	0.03	3
1984091	Agrini	4.35	2.60	0.15	2
1984122	Mundo	5.47	4.38	0.04	2
1984152	Caprock	5.61	4.51	0.09	3
1984207	Kappeli	5.62	4.40	0.10	3
1984215	Correo	4.57	2.91	0.06	4
1984243	Dolcetto	4.49	3.15	0.11	3
1984257	Breton	4.98	3.64	0.05	4
1984276	Vermejo	4.28	2.62	0.03	2
1984344	Egmont	5.51	4.32	0.12	4
1984350	Tierra	5.64	4.36	0.12	4
1985074	Vaughn	4.42	3.09	0.07	3
1985096	Misty Rain	4.7	3.44	0.08	4
1985122	Towanda	5.63	4.48	0.07	4
1985163	Salut	5.62	4.49	0.03	4
1985206	Serena	5.48	4.48	0.18	3
1985270	Ponil	4.49	3.15	0.10	4
1985282	Diamond Beech	4.01	2.42	0.09	4
1985289	Roquefort	4.62	3.07	0.06	4
1985339	Kinibito	5.6	4.26	0.06	3
1985362	Goldstone	5.45	4.28	0.01	4
1986081	Glencoe	5.41	3.74	0.09	3
1986100	Mighty Oak	4.93	3.52	0.05	2
1986112	Jefferson	5.48	4.42	0.14	3
1986141	Panamint	3.78	2.33	0.04	3
1986156	Tajo	5.29	4.18	0.00	1
1986176	Darwin	5.58	4.41	0.05	3
1986198	Cybar	5.57	4.51	0.02	3
1986205	Cornucopia	4.3	2.61	0.08	3
1986247	Galveston	3.71	2.50	0.08	2
1986273	Labquark	5.54	4.50	0.04	2
1986289	Belmont	5.56	4.52	0.05	3
1986318	Gascon	5.58	4.43	0.00	1
1986347	Bodie	5.52	4.55	0.00	1
1987042	Tornero	4.24	2.40	0.07	3
1987077	Middle Note	4.22	2.67	0.01	2
1987108	Delamar	5.51	4.40	0.07	3
1987120	Hardin	5.54	4.53	0.07	3
1987169	Brie	4.15	2.38	0.04	3
1987225	Tahoka	5.72	4.58	0.00	1
1987267	Lockney	5.61	4.60	0.07	2
1988046	Kernville	5.48	4.30	0.11	3
1988134	Schellbourne	4.77	3.36	0.03	3
1988142	Laredo	4.27	2.75	0.10	4
1988154	Comstock	5.58	4.34	0.02	2
1988189	Alamo	5.78	4.64	0.19	3
1988230	Kearsarge	5.64	4.41	0.10	4
1988243	Bullfrog	5.04	3.57	0.06	4
1988287	Dalhart	5.67	4.59	0.05	4
1988345	Misty Echo	4.79	3.48	0.00	1
1989041	Texarkana	5.32	3.99	0.02	3
1989055	Kawich-Red	4.41	2.47	0.14	3
1989068	Ingot	4.86	3.52	0.07	3
1989135	Palisade-1	4.55	2.71	0.07	3
1989146	Tulia	3.7	2.23	0.12	3
1989173	Contact	5.43	4.26	0.08	3
1989178	Amarillo	5.03	3.58	0.21	3
1989257	Disko Elm	4.04	2.40	0.17	4
1989304	Hornitos	5.83	4.40	0.09	4
1989342	Barnwell	5.56	4.19	0.16	4
1990069	Metropolis	5.16	3.66	0.03	4
1990164	Bullion	5.96	4.76	0.06	4
1990172	Austin	4.21	2.72	0.12	4
1990206	Mineral Quarry	4.53	3.23	0.18	4
1990318	Houston	5.46	4.13	0.05	4
1991067	Coso-Bronze	4.51	2.91	0.16	3
1991094	Bexar	5.65	4.36	0.04	3
1991257	Hoya	5.69	4.47	0.04	3
1991262	Distant Zenith	4.09	2.62	0.12	3
1991291	Lubbock	5.16	3.57	0.10	3
1991330	Bristol	4.79	3.35	0.17	3
1992086	Junction	5.81	4.16	0.31	3
1992175	Galena-Yellow	4.13	2.52	0.06	3
1992262	Hunters Trophy	4.16	2.59	0.12	3

gest that M_s and m_b will be fitted well by linear regressions, with approximately equal slopes assumed for the earthquake and explosion populations. Although we did observe slightly different slopes in the regression analyses for the two populations, we believe that this is due to inadequate sampling of earthquakes at m_b magnitudes greater than 5.2. Our dataset does not present any evidence that the two populations are converging at smaller magnitudes, although other M_s–m_b studies (Stevens and McLaughlin, 2001) suggest that convergence does occur. The classification equation based on the parallel-slope assumption becomes:

$$d = M_s(\mathrm{VMAX}) - 1.3m_b, \quad (7)$$

where d is the decision value. We chose to use the explosion slope because we believe that it is better constrained with the available data, and synthetic studies suggest (Bonner and Herrmann, 2004) that it does not change with increasing magnitude. If $d < -2.30$, the event will reside in the explosion population. We note that this does not require the event to be a nuclear explosion, because additional testing

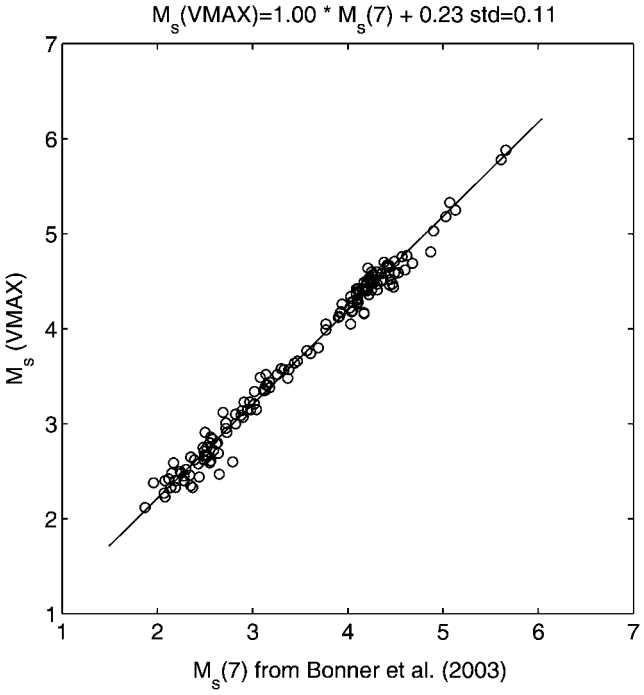

Figure 9. M_s(VMAX) magnitude estimates compared with 7-sec estimates based on a regionally calibrated Marshall and Basham formula. The M_s(VMAX) estimates result in a 25% reduction in variance as compared with the 7-sec estimates and are 0.25 m.u. larger.

is needed to ensure the event is shallow enough to be a candidate explosion. If $d > 2.30$, the event falls into the earthquake classification. We misclassified two earthquakes in the explosion population. In our previous studies based on 7-sec data (Bonner *et al.*, 2003), we misclassified four earthquakes as explosions.

Lop Nor Test Site Earthquake and Explosion Discrimination

In our third application of the Russell (2006) formula and M_s(VMAX) measurement technique, we examined earthquake and explosion discrimination at the Lop Nor nuclear test site in China.

Data. We developed a test dataset consisting of nine nuclear explosions and 38 earthquakes that occurred within 5 degrees of the Lop Nor test site. The broadband vertical-component data were acquired from IRIS and consisted of global and regional networks in the study region (Fig. 12). The data were all transformed from counts to displacement in nanometers using the SAC command "transfer" and SEED response files. The data were decimated from their original sampling rates (>20 samples/sec) to approximately 1 sample/sec for the surface-wave analysis. We do not have access to a calibrated body-wave magnitude scale for the Lop Nor region; thus, we have used the USGS-estimated m_b values in our discrimination analysis.

Results. Table 4 provides the M_s(VMAX) estimates and standard deviations for the explosions on the Lop Nor test site. The results for the earthquakes near the Lop Nor test site are compiled in Table 5. As shown in Figure 13, we regressed the M_s(VMAX) versus the USGS m_b for both the earthquake (Table 5) and explosion (Table 4) populations in our test dataset. The best-fitting regression lines are plotted as solid lines. The slope and intercepts for the lines are presented in the left subplot.

The slopes for the earthquake and explosion data were 1.0 and 1.2, respectively. Again, there is no evidence suggesting that the populations are converging at smaller magnitudes. We used the slope for the explosions to compute a

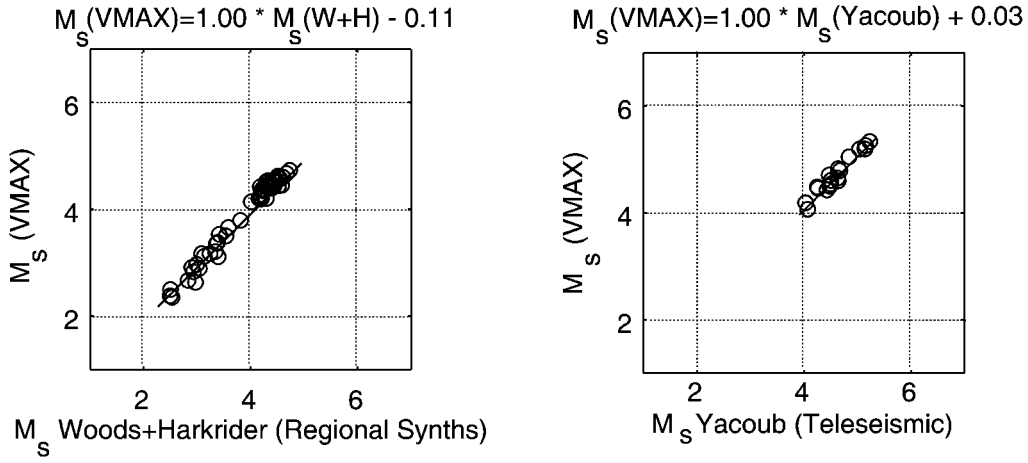

Figure 10. Fixed (slope = 1) regressions of M_s(VMAX) versus Woods and Harkrider (1995) (left) and Yacoub (1983) (right). The best-fitting regression line, with a fixed slope = 1.0, is given by the solid line running through the data points, and the offset is referenced in the equation above each plot.

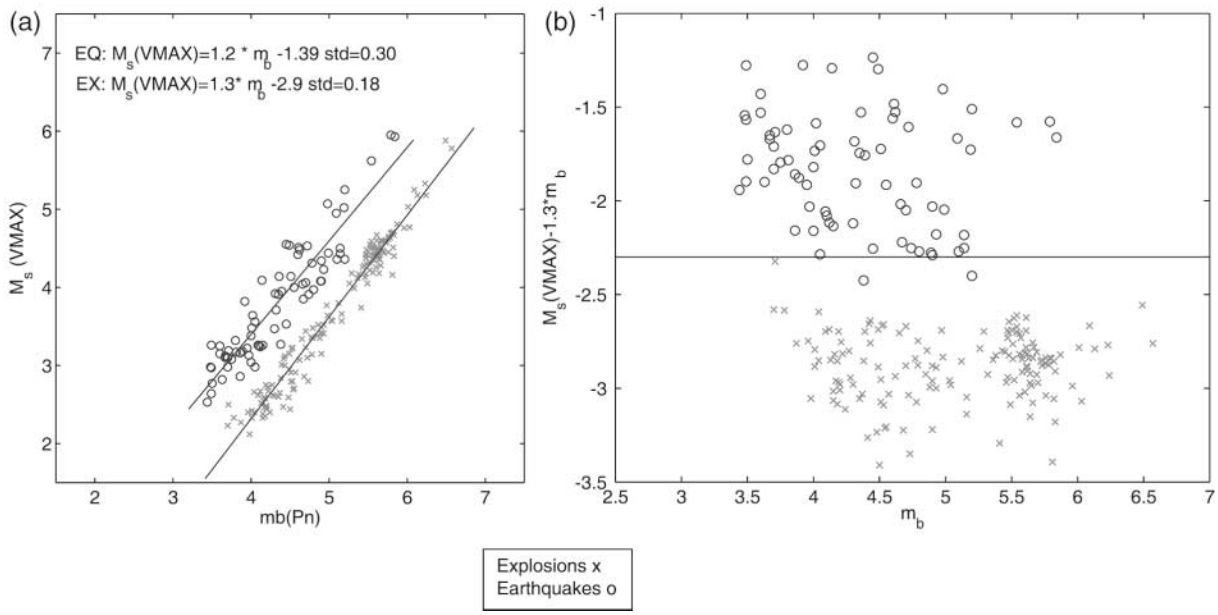

Figure 11. Discrimination results for M_s(VMAX) at the Nevada Test Site. (a) M_s (VMAX) versus m_b for western United States earthquakes and nuclear explosions. (b) Linear discrimination of the two datasets showing the decision line for classifying an event as a possible nuclear explosion. If $d = M_s(\text{VMAX}) - 1.3m_b$ is less than -2.30, the event may be an explosion, and additional analysis will be required to prove the event is not a deep and/or anomalous earthquake.

linear discriminant analysis. As a result, we developed the following classification equation:

$$d = M_s(\text{VMAX}) - 1.2m_b, \tag{8}$$

where d is the decision value. If $d < -2.6$, the event will reside in the explosion population and requires additional processing prior to being classified as a candidate explosion. If $d > -2.6$, the event falls into the earthquake classification. No Lop Nor explosions or earthquakes were misclassified using the VMAX magnitude estimation technique with the Russell (2006) surface-wave magnitude scale. However, we have fewer events for this region than we did for the NTS comparison.

Discussion

There is a general disagreement among researchers in the nuclear monitoring community as to how well the M_s–m_b discriminant performs at small-to-intermediate body-wave magnitudes. Some researchers believe that the available M_s–m_b datasets suggest that the two populations converge at smaller magnitudes (e.g., Stevens and McLaughlin, 2001). These researchers believe that the population convergence is caused by earthquake and explosion sources that become phenomenologically similar at smaller magnitudes. Lambert and Alexander (1971) determined that the earthquake and explosion populations at the Nevada Test Site are characterized by parallel M_s versus m_b curves, with slopes of 1 and a difference of 0.82 m.u. based on linear regression fits. Alexander (2002; personal comm., 2004) suggests that any convergence at the smaller magnitudes is related to depth and not the phenomenology behind explosion and earthquake sources.

To determine whether depth or source phenomenology is responsible for converging M_s–m_b behavior at smaller magnitudes, we pooled all of the Eurasian earthquake (Tables 1 and 5) M_s(VMAX) estimates. We also calculated M_s(VMAX) for 11 additional nuclear explosions in Eurasia (Table 6) and combined them with the Lop Nor explosions from Table 4. Figure 14 shows the M_s(VMAX) estimates from all these data plotted versus the USGS m_b.

Because of corner frequency effects for earthquakes and m_b measurement procedures, there should be a change in slope for regressed M_s(VMAX) versus m_b near m_b 5 (Nuttli, 1983). As shown in Figure 14, the slope for the best-fit regressions above m_b 5 is 1.46 with a standard deviation of 0.21 m.u. The slope for the regressions below m_b 5 is 0.94, which is similar to the slope determined for the observed explosion data (1.04). With the current dataset, we can not rule out the possibility that a single line with slope equal to 1.54 can fit all of the earthquake data. In fact, the correlation coefficients for single-line or two-line fits are essentially the same ($R^2 > 0.85$). If the earthquake data were fit with a single line, we would see convergence of the populations near m_b 3.5, which agrees with Stevens and McLaughlin (2001).

If we focus on the two-line case, however, the slopes

Table 3
Origin Information and M_s(VMAX) Test Results for Earthquakes in the Nevada Test Site Region

Year	Month	Day	Hour	Minute	Second	Latitute	Longitude	Depth	m_b	M_s (VMAX)	STD	No.
1979	08	12	11	31	19	37.26	−115.08	5.0	3.18	2.67	0.12	3
1979	12	25	00	0	00	37.27	−117.06	5.0	3.67	3.12	0.07	4
1980	01	15	20	28	22	36.18	−117.60	8.0	3.63	2.82	0.12	3
1980	02	25	23	43	32	36.20	−117.58	5.0	3.86	2.86	0.18	4
1980	05	27	14	50	57	37.48	−118.81	13.0	5.79	5.95	0.31	4
1981	12	01	16	18	50	38.62	−118.19	11.0	4.02	3.64	0.14	2
1981	12	19	20	56	52	38.63	−118.21	17.0	4.12	3.24	0.12	3
1982	01	24	15	44	07	37.45	−117.83	5.0	4.09	3.26	0.09	4
1982	03	16	08	47	00	36.60	−117.03	6.0	3.48	2.98	0.06	3
1982	05	12	19	29	24	37.27	−115.08	10.0	3.49	2.97	0.08	4
1982	07	06	02	10	43	37.69	−115.05	3.0	4.3	3.47	0.05	3
1982	09	24	07	40	24	37.85	−118.12	5.0	4.99	4.44	0.16	4
1983	06	04	11	37	40	37.39	−115.21	6.0	3.44	2.53	0.16	4
1984	08	02	11	1	34	37.30	−114.94	5.0	3.49	2.64	0.13	4
1984	11	23	18	8	25	37.48	−118.66	5.0	5.54	5.62	0.20	4
1985	12	10	06	10	25	37.30	−115.01	5.0	3.7	3.10	0.07	2
1992	06	29	10	31	02	36.69	−116.24	5.0	4.66	4.04	0.05	2
1992	06	29	15	52	39	36.71	−116.29	7.9	3.89	3.18	0.31	2
1992	06	29	17	1	16	36.74	−116.29	7.6	3.81	3.17	0.03	2
1992	06	30	16	6	24	36.72	−116.26	5.0	3.5	2.77	0.47	2
1992	07	05	06	54	12	36.69	−116.28	5.0	4.38	3.27	0.27	2
1993	05	17	23	20	49	37.17	−117.78	6.0	5.84	5.93	0.35	3
1993	05	18	01	3	06	37.15	−117.76	2.0	4.9	4.08	0.29	4
1993	05	18	23	48	53	37.06	−117.78	3.0	4.93	4.23	0.22	4
1993	05	20	20	14	14	36.10	−117.70	0.0	4.32	3.71	0.14	2
1995	06	26	08	40	27	34.31	−118.73	7.0	4.72	4.53	0.24	9
1995	08	17	22	39	58	35.75	−117.66	4.7	5.09	4.95	0.20	12
1995	08	30	15	54	22	35.73	−117.59	3.4	3.67	3.10	0.23	9
1995	09	20	23	27	36	35.69	−117.64	5.0	4.98	5.07	0.2	12
1995	09	22	14	47	22	38.70	−118.54	17.9	4.80	3.97	0.13	6
1996	01	07	14	32	53	35.72	−117.65	2.1	4.45	4.55	0.19	13
1996	01	08	08	57	10	35.76	−117.57	0.7	3.75	3.08	0.17	9
1996	01	08	10	52	29	35.75	−117.57	5.1	3.92	3.82	0.29	10
1996	04	02	01	50	09	37.60	−118.91	7.1	4.05	3.56	0.14	8
1996	05	01	19	49	56	34.33	−118.75	22.3	4.00	3.38	0.23	10
1996	06	02	07	0	06	39.09	−115.37	63.4	3.49	3.26	0.16	7
1996	11	27	20	17	24	36.01	−117.62	5.0	5.14	4.50	0.15	13
1997	04	14	11	20	54	38.09	−118.72	0.0	4.00	3.04	0.18	7
1997	05	06	19	12	53	35.43	−118.43	11.0	3.70	2.98	0.15	8
1997	07	03	17	49	36	35.77	−117.61	0.3	3.97	3.13	0.17	11
1997	08	21	16	11	24	38.55	−118.50	5.1	4.55	4.00	0.14	8
1997	08	21	16	36	47	38.56	−118.51	9.4	4.67	3.85	0.14	8
1997	11	02	08	51	54	37.81	−118.18	5.5	5.19	5.02	0.19	7
1997	11	02	15	3	04	37.85	−118.19	5.0	4.51	4.14	0.2	7
1997	11	05	23	0	08	37.20	−117.85	4.7	4.45	3.53	0.04	7
1997	11	15	06	0	20	37.18	−117.81	5.0	4.61	4.51	0.10	8
1997	11	22	12	6	57	37.63	−118.96	8.4	4.14	4.09	0.16	8
1997	11	22	17	20	37	37.64	−118.99	7.0	4.49	4.54	0.18	7
1997	11	22	18	11	01	37.63	−118.99	8.1	4.35	3.91	0.25	8
1997	11	30	21	17	07	37.57	−118.99	7.1	4.62	4.48	0.22	7
1997	12	31	20	36	49	37.65	−118.85	6.6	4.78	4.31	0.10	6
1998	03	06	07	36	34	36.01	−117.63	2.1	4.15	3.26	0.10	6
1998	03	07	00	36	46	36.00	−117.56	1.7	4.74	3.91	0.19	8
1998	04	24	16	17	27	38.49	−118.38	9.8	4.01	3.48	0.13	7
1998	06	09	05	24	41	37.59	−118.81	6.7	5.14	4.43	0.19	5
1998	06	18	11	0	41	37.96	−112.55	2.1	3.80	3.32	0.14	6
1998	07	02	03	39	51	36.82	−117.48	7.1	5.20	4.36	0.02	4
1998	07	15	04	53	21	37.55	−118.81	16.9	4.90	4.34	0.17	8
1999	01	27	10	44	23	36.84	−115.97	0.5	4.36	4.14	0.24	7
1999	05	15	13	22	12	37.49	−118.81	5.8	5.20	5.25	0.21	8

(*continued*)

Table 3
Continued

Year	Month	Day	Hour	Minute	Second	Latitute	Longitude	Depth	m_b	M_s (VMAX)	STD	No.
1999	05	15	17	54	10	37.51	−118.84	8.0	4.89	4.08	0.33	7
1999	05	17	06	37	20	37.54	−118.80	3.6	3.86	3.16	0.18	8
1999	08	01	16	27	20	37.35	−117.05	26.4	4.70	4.06	0.17	8
1999	08	02	05	40	27	37.39	−117.06	1.8	3.60	3.25	0.14	6
1999	08	02	06	5	14	37.30	−117.06	14.8	5.10	4.36	0.27	10
1999	11	08	01	53	13	37.40	−118.60	5.0	3.60	3.15	0.16	7
2001	05	17	21	53	45	35.73	−118.02	4.2	4.05	2.98	0.08	8
2001	07	17	12	59	59	35.95	−117.90	0.4	4.60	4.42	0.17	9
2001	08	02	16	21	19	37.22	−117.79	9.0	3.95	3.22	0.12	4
2002	06	14	12	40	44	36.72	−116.30	11.9	4.31	3.92	0.17	5
2002	09	28	10	34	47	35.95	−117.30	3.7	4.10	3.25	0.21	7
2003	01	25	09	16	10	35.32	−118.65	5.6	4.39	3.95	0.30	6
2003	03	08	15	35	02	37.57	−118.89	5.5	3.71	3.19	0.18	5

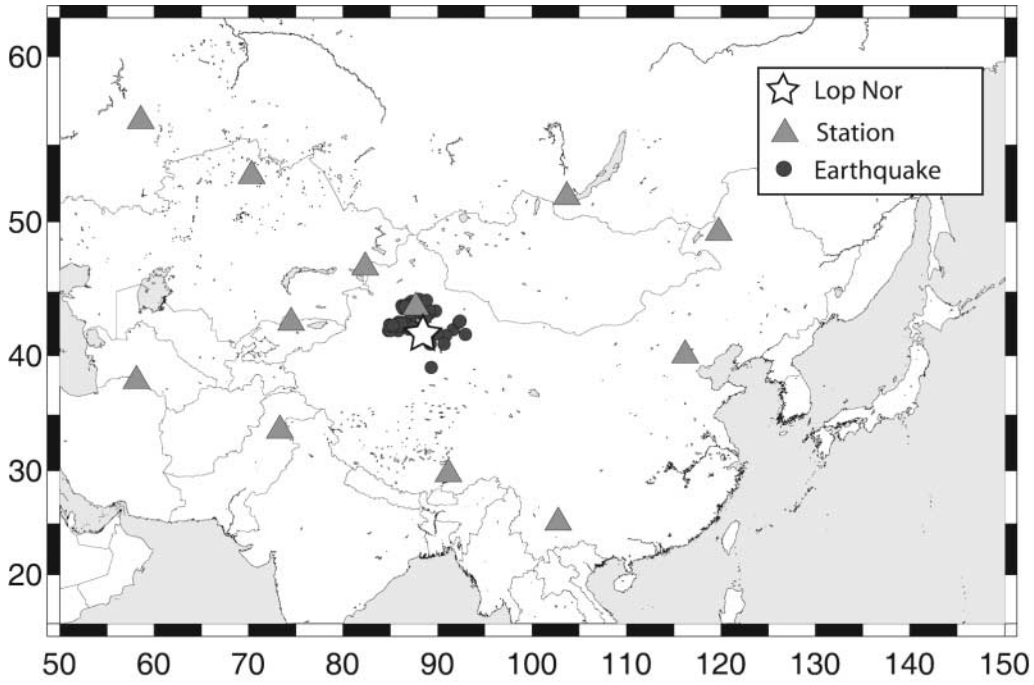

Figure 12. Test dataset consisting of Lop Nor explosions recorded on regional and near-teleseismic stations (filled triangles) together with western Chinese earthquakes (filled circles).

Table 4
Origin Information and M_s(VMAX) Test Results for Explosions at Lop Nor

Year	Month	Day	Hour	Minute	Second	Latitude	Longitude	Depth	m_b	M_s (VMAX)	STD	No.
1992	05	21	04	59	47	41.51	88.77	0	6.5	5.06	0	1
1992	09	25	07	59	58	41.72	88.34	0	5	2.98	0	1
1993	10	05	01	59	56	41.67	88.70	0	5.9	4.09	0.24	3
1994	06	10	06	25	57	41.53	88.71	0	5.8	3.51	0	1
1994	10	07	03	25	58	41.66	88.75	0	6	4.02	0.08	6
1995	05	15	04	05	57	41.60	88.82	0	6.1	4.13	0.19	6
1995	08	17	00	59	57	41.56	88.80	0	6	4.15	0.13	6
1996	06	08	02	55	58	41.66	88.69	0	5.9	4.07	0.1	7
1996	07	29	1	48	57	41.82	88.42	0	4.9	3.01	0.18	5

Table 5
Origin Information and M_s(VMAX) Test Results for Earthquakes Near Lop Nor

Year	Month	Day	Hour	Minute	Second	Latitude	Longitude	Depth	m_b	M_s (VMAX)	STD	Stations
1995	08	02	11	59	43	41.63	88.45	10	4.1	3.32	0	1
1995	09	04	18	43	45	43.90	87.44	33	4.1	2.91	0.13	5
1995	12	12	17	31	16	42.12	86.91	33	4.3	3.32	0.2	6
1996	03	04	14	02	22	44.12	87.20	33	3.9	3.22	0.07	4
1996	03	20	02	11	21	42.18	87.63	24	4.8	3.76	0.2	9
1996	03	31	03	07	14	43.02	88.68	33	4.2	3.24	0.21	6
1996	05	12	01	00	38	43.67	86.96	33	3.7	2.95	0.22	2
1997	02	08	17	12	09	42.34	86.99	9	4.6	3.54	0.35	2
1997	05	27	01	56	24	42.62	86.16	21	4.9	3.64	0.14	7
1997	06	08	20	25	53	39.06	89.28	33	4.7	3.2	0.17	7
1998	01	20	19	35	04	42.01	84.75	33	3.5	2.75	0	1
1998	02	07	22	42	44	42.55	86.01	33	4.1	3.1	0.11	3
1998	04	13	23	14	32	41.99	85.80	33	4	2.92	0.28	2
1998	08	19	12	26	19	43.81	86.33	19	4.6	3.71	0.2	9
1998	10	20	18	39	23	42.56	87.15	33	4.7	3.2	0.12	7
1999	01	27	06	25	01	41.62	88.36	33	4.5	3.36	0.16	8
1999	01	30	03	51	05	41.67	88.46	23	5.9	5.25	0.14	6
1999	04	29	05	27	55	41.62	90.82	33	4.3	3.26	0.21	8
1999	05	01	13	48	52	42.04	87.96	21	4.2	2.96	0.21	5
1999	05	17	04	52	34	42.28	87.92	33	4.2	2.92	0.35	3
1999	10	18	02	42	20	41.77	89.25	33	5	4.25	0.15	8
2000	10	03	03	07	28	41.99	84.92	33	5.2	4.37	0.28	7
2001	03	13	03	18	38	42.39	86.12	24	4.7	3.67	0.11	9
2001	12	21	23	05	50	43.74	86.53	10	4.5	3.68	0.2	9
2002	01	13	05	27	16	43.36	89.04	33	4.3	3.22	0.18	9
2002	03	11	23	26	49	42.39	85.90	33	4.6	3.52	0.14	9
2002	10	02	09	50	52	43.57	89.08	29	4.6	3.32	0.06	3
2002	10	07	03	01	47	43.42	87.09	29	4.8	3.98	0.11	8
2003	01	22	13	33	02	42.21	87.33	24	4.7	3.33	0.23	9
2003	02	13	18	32	47	41.91	88.24	51	4.3	3.5	0.22	9
2003	02	23	22	34	20	43.75	87.71	33	4.2	3.13	0.22	9
2003	03	13	15	07	07	41.80	89.08	33	4.8	3.64	0.19	9
2003	07	03	05	53	52	43.85	86.26	37	4.8	4.09	0.21	7
2003	08	24	21	54	36	44.30	87.20	33	4.1	3.11	0.21	8
2003	12	19	15	01	22	41.95	88.85	33	4.7	3.82	0.18	3
2004	01	29	15	29	08	42.54	86.13	15	4.3	3.14	0.09	6
2004	03	20	22	55	03	43.87	86.50	10	4.1	3.25	0.14	3
2004	03	29	20	30	32	43.04	88.65	21	4.2	2.9	0.33	4

Table 6
Origin Information and M_s(VMAX) Test Results for Additional Eurasian Explosions

Year	Month	Day	Hour	Minute	Second	Latitude	Longitude	m_b	M_s (VMAX)	STD	No.	Test Site
1989	10	19	9	49	59	49.927	78.972	6	4.38	0.07	3	Shagan
1989	10	04	11	30	0	49.751	78.005	4.7	3.23	0	1	Shagan
1989	09	02	4	16	59	50.019	78.998	5.1	3.29	0.24	2	Shagan
1989	07	08	3	47	0	49.869	78.775	5.6	3.78	0.15	3	Shagan
1989	02	12	4	15	9	49.911	78.704	5.9	4.24	0	1	Shagan
1989	01	22	3	57	9	49.934	78.815	6.1	4.28	0	1	Shagan
1988	12	17	4	18	9	49.879	78.924	5.9	4.15	0	1	Shagan
1988	11	23	3	57	9	49.767	78.029	5.4	3.56	0	1	Shagan
1990	10	24	14	57	58	73.331	54.757	5.7	4.08	0.17	7	Novaya Zemlya
1998	05	11	10	13	44	27.078	71.719	5.2	3.17	0.11	8	India
1998	05	28	10	16	17	28.83	64.95	4.9	3.27	0.18	8	Pakistan

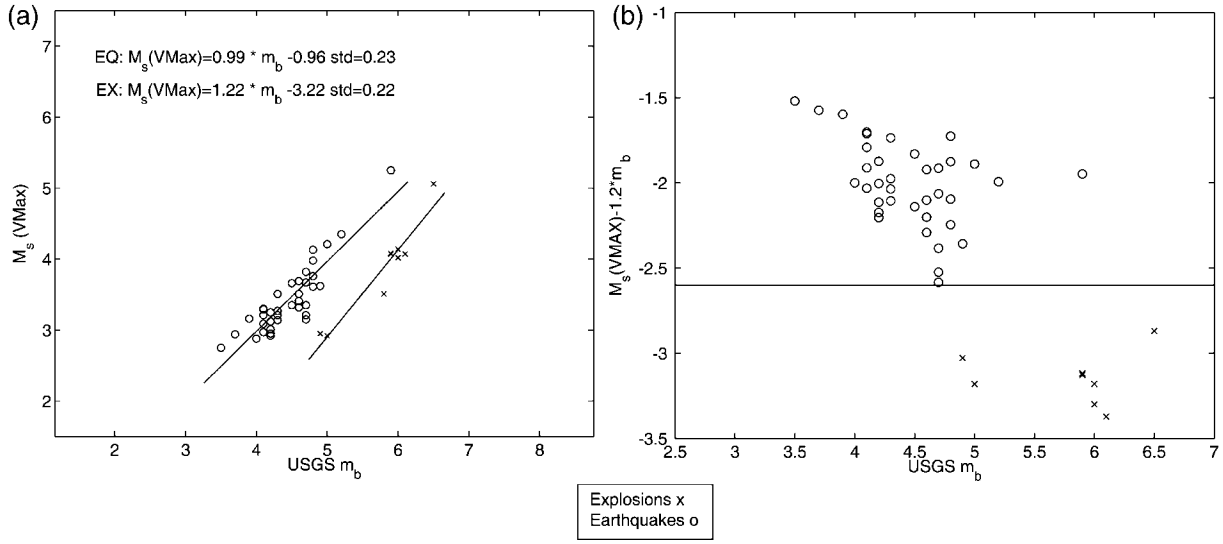

Figure 13. Discrimination results for M_s (VMAX) at the Lop Nor Test Site. (a) M_s (VMAX) versus m_b for earthquakes in northwestern China and nuclear explosions at Lop Nor. (b) Linear discrimination of the two datasets showing the decision line (-2.6) for classifying an event as a possible nuclear explosion.

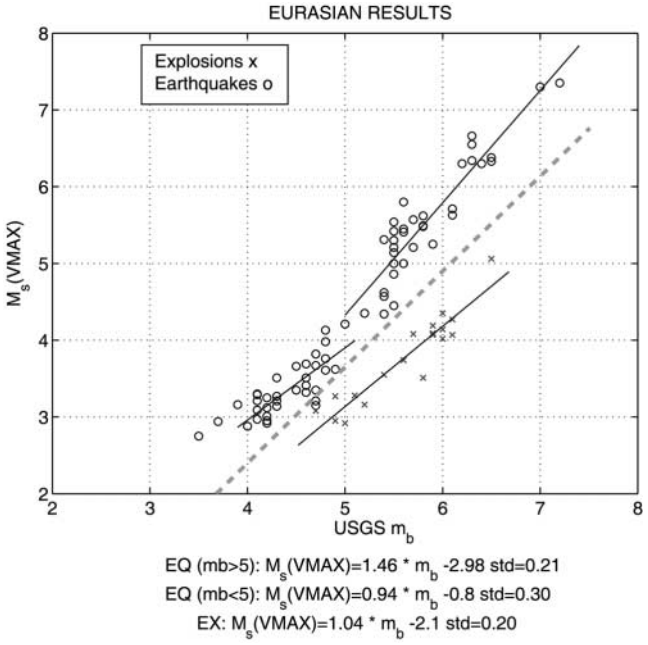

Figure 14. M_s–m_b relationships for all Eurasian earthquake and explosion data for which an M_s (VMAX) was estimated during this study. The body-wave magnitudes are all from the United States Geological Survey. We split the earthquake data at $m_b = 5$ based on corner frequency effects for earthquakes and m_b. The earthquake and explosion populations both have slopes that are approximately 1 for $m_b < 5$ and are separated by an average of 0.90 m.u. The dashed line is the Murphy *et al.* (1997) criterion for event screening.

for our earthquake and explosion populations at m_b values <5 are similar to the Lambert and Alexander (1971) results. Additionally, we observed 0.90 m.u. separation between the two populations at m_b values below 5, whereas Lambert and Alexander (1971) noted a difference of 0.82 m.u., based on the fitted regression lines for their NTS earthquakes and explosions. Although more data will be required to finalize the two-slope hypothesis, these preliminary results suggest that the discrimination of explosions from earthquakes can be achieved at lower magnitudes using the Russell (2006) formula and the M_s(VMAX) measurement technique.

Murphy *et al.* (1997) determined an event-screening relationship based on M_s–m_b estimates. For USGS-estimated m_b, the screening criterion is:

$$M_s = 1.25m_b - 2.60. \quad (9)$$

We plotted the Murphy *et al.* (1997) criterion in Figure 14 as the dashed line and note that two of the earthquakes fall below this line. More importantly, none of our explosions plotted above this line.

Conclusions

The Russell surface-wave magnitude formula and the M_s(VMAX) measurement technique provide a new method for estimating surface-wave magnitudes. The new method has several benefits. First, the technique allows for time-domain measurements of surface-wave amplitudes, giving an analyst the ability to visually confirm that the pick is

correct and is an actual surface wave. Also, it allows for surface-wave magnitudes to be measured at local and regional distances where traditional 20-sec magnitudes cannot be used. And these magnitudes are not biased with respect to teleseismic estimates using the same M_s(VMAX) measurement technique. Additionally, the application of narrowband Butterworth-filtering techniques appropriately handles Airy phase phenomena that, before this study, had to be accounted for by using Marshall and Basham's (1972) empirical corrections. Finally, because the method is variable period and not restricted to near 20-sec period, the analyst is allowed to measure M_s where the signal is largest. The new method has been successfully tested on three research datasets, and the results suggest that the method can be used to screen out a large percentage of small earthquakes at $m_b < 5$. Thus, we are currently implementing the technique for operational testing.

Acknowledgments

The data used in this study come from a variety of sources. We thank the following organizations for providing access to their data: the Geological Survey of Canada; Institut de Physique du Globe de Paris; GFZ Potsdam, Germany; U.S. Geological Survey, National Science Foundation, University of California, San Francisco; California Institute of Technology; Lamont Doherty Earth Observatory; and Istituto Nazionale di Geofisica e Vulcanologia, Rome, Italy. We are also indebted to Howard Patton for his assistance in the LNN database acquisition and his comments concerning various aspects of the research. We also thank Bill Walter and Marv Denny for help in acquiring the MNV dataset (Denny, 1998). We are grateful to Mark Leidig and Ileana Tibuleac, who helped with database preparation, and to Jack Murphy, Heather Hooper, and James Lewkowicz for insightful discussions about the article and research. Karl Veith and an anonymous reviewer helped improve the article during the review process. We thank the developers of the Generic Mapping Tools software (Wessel and Smith, 1998), Computer Programs in Seismology (Herrmann, 2004), and Matlab, all of which were used to generate and present the results of our research. We are also grateful to Harvard University for making their CMT estimates readily available. This research was sponsored by the U.S. Air Force Research Laboratory and the Defense Threat Reduction Agency under Contract DTRA01-01-C-0080

References

Alexander, S. S. (2002). Seismic monitoring for underground nuclear explosions, in *Science, Technology and National Security*, S. K. Majumbar, S. S. Alexander, L. M. Rosenfeld, M. F. Rieders, E. W. Miller, and A. I. Panah (Editors), The Pennsylvania Academy of Sciences, Easton, Pennsylvania, 267 pp.

Bonner, J., and R. B. Herrmann (2004). A Synthetic M_s–m_b study, Weston Geophysical Scientific Report, 20 pp.

Bonner, J., D. Harkrider, E. T. Herrin, R. H. Shumway, S. A. Russell, and I. M. Tibuleac (2003). Evaluation of short-period, near-regional M_s scales for the Nevada Test Site. *Bull. Seism. Soc. Am.* **93,** 1773–1791.

Bonner, J. L., D. T. Reiter, and D. Harkrider (2004). Development of a time-domain, variable-period surface wave magnitude measurement procedure for application at regional distances, in *Proc. of the 26th Annual Seismic Research Review Meeting*, Orlando, Florida.

Chael, E. P. (1997). An automated Rayleigh-wave detection algorithm, *Bull. Seism. Soc. Am.* **87,** 157–163.

Denny, M. D. (1998). Mina seismic data: historic background for CTBT monitoring, Lawrence Livermore Report UCRL-MI-130657.

Denny, M. D., S. R. Taylor, and E. S. Vergino (1987). Investigation of m_b and M_s formulas for the western United States and their impact on the M_s/m_b discriminant, *Bull. Seism. Soc. Am.* **77,** 987–995.

Denny, M. D., S. R. Taylor, and E. S. Vergino (1989). Erratum: investigation of m_b and M_s formulas for the western United States and their impact on the M_s/m_b discriminant, *Bull. Seism. Soc. Am.* **79,** 230.

Dziewonski, A. M., J. Bloch, and M. Landisman (1969). A new technique for the analysis of transient seismic signals, *Bull. Seism. Soc. Am.* **59,** 427–444.

Gutenberg, B. (1945). Amplitudes of surface waves and the magnitudes of shallow earthquakes, *Bull. Seism. Soc. Am.* **35,** 3.

Herak, M., and D. Herak (1993). Distance dependence of M_s and calibrating function for 20 second Rayleigh waves, *Bull. Seism. Soc. Am.* **83,** 1681.

Herrmann, R. B. (2004). Computer Programs in Seismology Version 3.30, St. Louis University, St. Louis, Missouri.

Kanamori, H., and G. S. Stewart (1976). Mode of strain release along the Gibbs Fracture Zone, Mid-Atlantic Ridge, *Phys. Earth Planet. Interiors* **11,** 312–332.

Lambert, D. G., and S. S. Alexander (1971). Relationship of body and surface wave magnitudes for small earthquakes and explosions, SDL Report 245, Teledyne Geotech, Alexandria, Virginia.

Marshall, P. D., and P. W. Basham (1972). Discrimination between earthquakes and underground explosions employing an improved M_s scale, *Geophys. J. R. Astr. Soc.* **29,** 431–458.

Murphy, J. R., B. W. Barker, and M. E. Marshall (1997). Event screening at the IDC using the Ms/mb discriminant, Maxwell Technologies Final Report, 23 pp.

Nuttli, O. W. (1983). Average seismic source-parameter relations for mid-plate earthquakes, *Bull. Seism. Soc. Am.* **73,** 519–535.

Okal, E. A. (1989). A theoretical discussion of time domain magnitudes: the Prague formula for M_s and the mantle magnitude M_m, *J. Geophys. Res.* **94,** 4194–4204.

Patton, H. (2001). Regional magnitude scaling, transportability, and M_s-m_b discrimination at small magnitudes, in *Monitoring the Comprehensive Nuclear Test Ban Treaty: Source Processes and Explosion Yield Determination*, G. Ekstrom, M. Denny, and J. R. Murphy (Editors), *Pure Appl. Geophys.* **158,** 1951–2015.

Rezapour, M., and R. G. Pearce (1998). Bias in surface-wave magnitude M_s due to inadequate distance correction, *Bull. Seism. Soc. Am.* **88,** 43–61.

Russell, D. R. (2006). Development of a time-domain, variable-period surface wave magnitude measurement procedure for application at regional and teleseismic distances, part I: theory, *Bull. Seism. Soc. Am.* **96,** no. 2, 665–677.

Selby, N. (2001). Association of Rayleigh waves using back azimuth measurements: application to test ban verification, *Bull. Seism. Soc. Am.* **91,** 580–593.

Stevens, J. L., and S. M. Day (1985). The physical basis of the mb:Ms and variable frequency magnitude methods for earthquake/explosion discrimination, *J. Geophys. Res.* **90,** 3009–3020.

Stevens, J. L., and K. L. McLaughlin (2001). Optimization of surface wave identification and measurement, in *Monitoring the Comprehensive Nuclear Test Ban Treaty: Surface Waves*, A. Levshin and M. H. Ritzwoller (Editors), *Pure Appl. Geophys.* **158,** 1547–1582.

Stevens, J. L., D. A. Adams, and E. Baker (2001). Surface wave detection and measurement using a one-degree global dispersion grid, SAIC Final Report SAIC-01/1085.

Vaněk, J., A. Zatopek, V. Karnik, Y. V. Riznichenko, E. F. Saverensky, S. L. Solov'ev, and N. V. Shebalin (1962). Standardization of magnitude scales, *Bull. Acad. Sci. U.S.S.R., Geophys. Ser.* **2,** 108 (in English).

Vergino, E. S., and R. W. Mensing (1989). Yield estimation using regional $m_b(Pn)$, Lawrence Livermore National Laboratory Report UCID-101600.

von Seggern, D. (1977). Amplitude distance relation for 20-second Rayleigh waves, *Bull. Seism. Soc. Am.* **67,** 405–411.

Wessel, P., and W. H. F. Smith (1998). New, improved version of the Generic Mapping Tools Released, *EOS*, *Trans. AGU* **79,** 579.

Woods, B., and D. G. Harkrider (1995). Determining surface-wave magnitudes from regional Nevada Test Site data, *Geophys. J. Int.* **120,** 474–498.

Yacoub, N. K. (1983). Instantaneous amplitudes: a new method to measure seismic magnitude, *Bull. Seism. Soc. Am.* **73,** 1345–1355.

Weston Geophysical Corporation
4000 S. Medford Suite 10W
Lufkin, Texas 75904
bonner@westongeophysical.com
(J.L.B.)

Air Force Technical Applications Center
Patrick Air Force Base, Florida
(D.R.R.)

Weston Geophysical Corporation
57 Bedford Street, Suite 102
Lexington, Massachusetts 02420
hark@ourconcord.net
delaine@westongeophysical.com
(D.G.H., D.R.)

Department of Earth & Atmospheric Sciences
Saint Louis University
3507 Laclede Avenue
St. Louis, Missouri 63103
rbh@eas.slu.edu
(R.B.H.)

Manuscript received 21 March 2005.